

## Endothelial injury, F-actin and vitamin D binding protein after hematopoietic stem cell transplant and association with clinical outcomes

Nathan Luebbering,<sup>1,2</sup> Sheyar Abdullah,<sup>1,2</sup> Dana Louder,<sup>1,2</sup> Adam Lane,<sup>1,2</sup> Nikhil Dole,<sup>1,2</sup> Jeremy Rubinstein,<sup>1,2</sup> Martin Hewison,<sup>2</sup> Nicholas Gloude,<sup>1,2</sup> Sonata Jodele,<sup>1,2</sup> Kitty MR Perentesis,<sup>1,2</sup> Kelly Lake,<sup>1,2</sup> Bridget Litts,<sup>1,2</sup> Alexandra Duell,<sup>1,2</sup> Christopher E. Dandoy<sup>1,2</sup> and Stella M. Davies<sup>1,2</sup>

<sup>1</sup>Division of Bone Marrow Transplantation and Immune Deficiency, Cincinnati Children's Hospital Medical Center Cincinnati, OH, USA; <sup>2</sup>Department of Pediatrics, University of Cincinnati, Cincinnati, OH, USA and <sup>3</sup>School of Clinical and Experimental Medicine, College of Medical and Dental Sciences, University of Birmingham, Birmingham, UK

©2021 Ferrata Storti Foundation. This is an open-access paper. doi:10.3324/haematol.2019.233478

Received: July 25, 2019.

Accepted: March 19, 2020.

Pre-published: April 2, 2020.

Correspondence: *STELLA M. DAVIES* - stella.davies@cchmc.org

---

## Supplemental Materials, Luebbering et al.

### Supplemental Methods

*Calculation of Bioavailable 25-Hydroxyvitamin D* Free vitamin D is defined as circulating 25-OH D not bound to VDBP, but does include the albumin bound fraction. Free vitamin D levels were calculated from measurements of total serum 25-OH-D<sub>2</sub>, 25-OH-D<sub>3</sub>, and DBP using previously documented equations that incorporate both genotype-specific and genotype-nonspecific affinity constants.

*Measurement of ATP Levels by Quantitative Mass Spectrometry* Samples were prepared from 10  $\mu$ L of plasma by precipitation of proteins with a 3 volume cold acetone followed by centrifugation and injection of 15  $\mu$ L of supernatant per sample. ATP quantitation was performed by LC-MS-SRM using a Shodex HILICpak VN-50 2D column, 5  $\mu$ m, 2.1 mm X 150 mm column, (New York, NY) on a Vanquish™ Flex Quaternary UHPLC system (Thermo Fisher Scientific, San Jose, CA) coupled to a Thermo Scientific™ Quantiva™ triple quadrupole mass spectrometer by negative ion mode electrospray ionization and selected reaction monitoring (SRM) mass spectrometry using diagnostic transitions for ATP. A stock solutions of ATP was prepared and infused into the QQQ mass spectrometer for optimization of precursor transition as well as product ion fragmentation. To enhance detection specificity for ATP, the precursor at m/z 505.9 was monitored as two SRM transition fragment ions at 159 and 408 using collision energies of 29 and 17 volts, respectively.

The separation Mobile phase A consisted of acetonitrile (Honeywell Burdick & Jackson, Morris Plains, NJ) Mobile phase B consisted of a 50 mM ammonium bicarbonate and with a gradient of 15% B (from 0 to 4 min) increasing to 35% B at 6 min, 75% B at

6.5 min (hold for 1 min), 15% B at 7.6 min, holding for 12.4 min for equilibration at a flow rate of 300  $\mu\text{L min}^{-1}$ . The column temperature was set at 60 °C. ATP signal intensity (arbitrary units) was monitored across the LC-MS-SRM run and the peak areas for the specific SRM transitions were captured versus retention time. The quantitative data are reported as peak areas of the SRM intensities across the chromatographic run.

### *VDBP Glycosylation Studies*

Protein concentration of each sample was determined by Qubit fluorometry. 10 $\mu\text{L}$  of protein from each sample was depleted in duplicate on a Pierce Top 12 depletion spin cartridge according to manufacturer's protocol. Depleted samples were buffer exchanged into water on a Corning Spin X 5kD molecular weight cut off spin column and quantified by Qubit fluorometry (Life Technologies). 50 $\mu\text{g}$  of each sample was reduced with dithiothreitol, alkylated with iodoacetamide and digested overnight with trypsin (Promega); digestion was terminated with formic acid. Each digested sample was processed by solid phase extraction using an Empore C18 (3M) plate under vacuum (5in Hg) with the following protocol: Columns were activated with 400 $\mu\text{L}$  95% acetonitrile/0.1% TFA X2 and equilibrated with 400 $\mu\text{L}$  0.1% TFA X4. Acidified samples were loaded and columns washed with 400 $\mu\text{L}$  0.1% TFA X2. Peptides were eluted with 200 $\mu\text{L}$  70% acetonitrile/0.1% TFA X2 and lyophilized for further processing. Half of each gel digest was analyzed by nano LC-MS/MS with a Waters NanoAcquity HPLC system interfaced to a ThermoFisher Q Exactive. Peptides were loaded on a trapping column and eluted over a 75 $\mu\text{m}$  analytical column at 350nL/min with a 1hr reverse phase gradient; both columns were packed with Luna C18 resin (Phenomenex). The mass spectrometer was operated in data-dependent mode, with the Orbitrap operating

at 60,000 FWHM and 17,500 FWHM for MS and MS/MS respectively. The fifteen most abundant ions were selected for MS/MS.

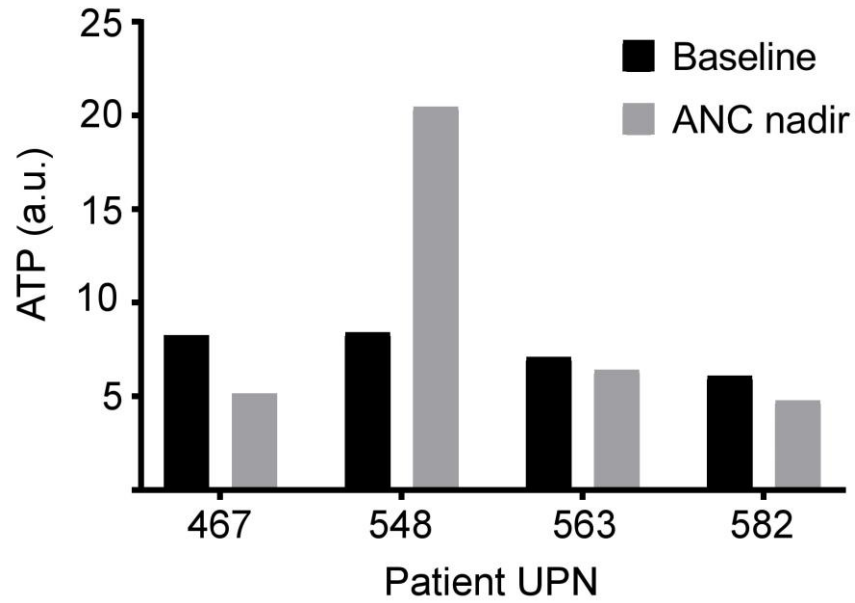
**Supplemental Table 1.**

<b>Gene</b>	<b>Function</b>	<b>Change with increased DBP</b>
SIGLEC-1 (CD169)	Macrophage marker, induced by TLR agonists (35)	Increased 8.3 fold
ADORA3	Adenosine A1 receptor; macrophage gene that regulates IL6 and TNF production and suppress IL12 (36)	Increased 8.2 fold
IL1R2	Interleukin 1 receptor, type II; expression increased in M2 macrophages (37)	Increased 7.7 fold
SH3PXD2B	LPS suppresses the phagocytic function of macrophages by down-regulation of SH3PXD2B expression through TLR4 pathway (38)	Increased 7.2 fold
TMIGD3	Encodes a transmembrane and immunoglobulin domain-containing protein that has overlapping activities with ADORA3 (39)	Increased 6.5 fold
IFI44L	IFN1 signature gene (40)	Increased 6.4 fold
SERPINB2	M2 "specific" marker (41)	Increased 6.2 fold
IFIT3	Part of IFN1 signature, induced by and active against viruses (40)	Increased 6.2 fold
C1QB	Marker of macrophage activation (42)	Increased 6.1 fold
IFI6	IFN1 signature gene (40)	Increased 5.3 fold
MARCO (macrophage receptor with collagenous structure)	Macrophages need MARCO to bind bacteria and this activity is impaired by free actin. Actin scavenging has been linked to MARCO activity. (42, 43)	Increased 4.8 fold
IL6	Produced by macrophages after stimulation by the anti-inflammatory cytokine IL-4. (42)	Increased 4.6 fold
CCL22	Expression increased in M2 macrophages (44)	Reduced 0.6 fold
CCL5	Expressed in M1 macrophages (45)	Reduced 0.44 fold
CLEC4A	Expression increased in M2 macrophages (46)	Reduced 0.28 fold
MMP9	Expression increased in M2 macrophages (46)	Reduced 0.1 fold

**Supplemental Table 1:** Genes with most altered expression after incubation of normal peripheral blood mononuclear cells with serum collected from transplant recipients 100 days after HSCT compared with serum collected at day 0.

Glycan (mean AUC)	Genotype Gc1/Gc1			Genotype Gc2/Gc1		
	Day 0	Day 100	p-value (day 0 vs day 100)	Day 0	Day 100	p-value (day 0 vs day 100)
HexNAc	6,283,000	3,518,000	0.1093	5,176,000	5,082,000	0.9709
HexNAc(1)Hex(1)	2,769,000	2,668,000	0.8719	1,160,000	1,607,000	0.5286
HexNAc(1)Hex(1)NeuAc(1)	126,755,000*	117,640,000*	0.4773	68,016,000*	82,989,000*	0.5420
HexNAc(1)Hex(1)NeuAc(2)	<b>2,291,000</b>	<b>1,666,000</b>	<b>0.0099</b>	3,117,000	1,552,000	0.1604

**Supplemental Table 2:** Glycosylation of VDBP determined by mass spectroscopy in serum samples from 2 individuals of genotypes Gc1/Gc1 and Gc2/Gc1, comparing samples collected at day 0 and day 100 after HSCT. The Gc2 allele is not glycosylated with the trisaccharide (HexNAc(1)Hex(1)NeuAc(1)) as the threonine base is replaced with lysine, so the level of the dominant glycan is approximately half that seen in those with two Gc1 alleles as expected, (compare values marked with an asterisk;  $p = 0.004$ ). No significant change in glycosylation of the major glycan is seen in either individual between day 0 and 100.



**Supplemental Figure 1:** ATP levels measured by mass spectrometry in samples collected from four HSCT recipients prior to BMT and at time of ANC nadir (maximum cell lysis). The bars demonstrate area of peak intensity from the SRM transition of each nucleoside phosphate as denoted in the methods section.